AIMS Mathematics, 11(1): 558–577.
DOI: 10.3934/math.2026024
Received: 14 November 2025
Revised: 22 December 2025
Accepted: 26 December 2025
Published: 08 January 2026

http://www.aimspress.com/journal/Math

Research article

Dynamics of an HIV model with immune response and two types of infected cells

Weimiao Zheng, Juan Wang* and Xia Wang

School of Mathematics and Statistics, Xinyang Normal University, Xinyang 464000, Henan, China

* **Correspondence:** Email: dotey99@126.com.

Abstract: This research investigates a mathematical model for human immunodeficiency virus (HIV) infections that incorporates cytotoxic T lymphocyte (CTL) immune responses and two types of infected cells. Additionally, the model reflects the effect of antiretroviral therapies. By using the next-generation matrix method, the basic reproduction number R_0 and the CTL immune reproduction number R_1 are calculated. The existence and stability of equilibria are discussed. In particular, if $R_0 < 1$, then the infection-free equilibrium is globally asymptotically stable. Moreover, through analyzing the transmission dynamics of HIV within the human body under the influence of drug treatment, this study provides a theoretical foundation to optimize antiretroviral therapy strategies.

Keywords: HIV infection model; two types of infected cells; cell-to-cell transmission; basic reproduction number; CTL immune response
Mathematics Subject Classification: 34D23, 92D30

1. Introduction

The human immunodeficiency virus (HIV) primarily targets $CD4^+$ T lymphocytes. HIV infection ultimately leads to the gradual collapse of the patient's immune system, which results in acquired immunodeficiency syndrome (AIDS) [1]. The process of HIV infection is complex and dynamic, involving multiple components and cell types of the human immune system [2]. HIV enters susceptible cells through specific receptors and co-receptors, such as the CD4 receptor, which reside on the surface of target cells. After binding these receptors on the target cell surface, the virus releases its core material into the cell through membrane fusion. Inside the cell, the viral RNA is reverse-transcribed into DNA, which is then integrated into the host cell's genome to form a provirus. The provirus can remain latent within the cell or undergo active replication, thus producing new viral particles [3]. During the early stages of infection, the body's non-specific immune response is first activated, thereby recognizing and clearing some infected cells. Subsequently, specific antibodies are

produced that bind to viral particles, thus preventing further infection of other cells and modulating the immune response to promote viral clearance. As the infection progresses, the number of $CD4^+$ T lymphocytes gradually decreases, and eventually leads to severely impaired cellular immune function and immunodeficiency [4].

As mentioned in [5], a time-adaptive finite element method was developed to tackle the parameter identification problem for the following system of ODEs, which describe the dynamics of HIV infection with drug therapy:

$$\begin{cases} \dfrac{du_1}{dt} &= f_1(u(t), \eta(t)) = s - ku_1(t)u_4(t) - \mu u_1(t) + (\eta(t)\alpha + b)u_2(t), \\ \dfrac{du_2}{dt} &= f_2(u(t), \eta(t)) = ku_1(t)u_4(t) - (\mu_1 + \alpha + b)u_2(t), \\ \dfrac{du_3}{dt} &= f_3(u(t), \eta(t)) = (1 - \eta(t))\alpha u_2(t) - \delta u_3(t), \\ \dfrac{du_4}{dt} &= f_4(u(t), \eta(t)) = N\delta u_3(t) - cu_4(t), \end{cases} \tag{1.1}$$

where $u_1(t)$, $u_2(t)$, $u_3(t)$, and $u_4(t)$ represent the population sizes of uninfected target cells, infected target cells before reverse transcription, infected target cells after completed reverse transcription, and free virus particles, respectively. The values of the remaining model parameters are adopted from [5]; the study employed a local time-mesh refinement algorithm to identify the time-varying parameter of drug efficacy, thus demonstrating its effectiveness and robustness.

In addition to standard virus-to-cell infections, alternative transmission modes significantly influence viral dynamics. Cell-to-cell transmission can facilitate the spread and immune evasion, as shown in models such as [6–8]. In [9], the authors developed and analyzed a stochastic HIV model with dual infection modes and delays, revealing how noise intensity critically determines viral persistence or extinction. Guo et al. [10] further integrated antiretroviral therapies and latent reservoirs, and revealed that CTL efficacy is crucial to achieve a functional cure even under potent drug treatment, and that cell-to-cell transmission can undermine therapeutic outcomes. Furthermore, the infection process can be modulated by the host's immune environment. Regarding cytokine-enhanced viral infection, as explored by Wang et al. [11], illustrates how inflammatory signals (e.g., from pattern recognition receptors) can upregulate viral receptors on target cells, thereby creating a positive feedback loop that exacerbates infection.

The role of cytotoxic T lymphocyte (CTL) responses in controlling HIV infection has been extensively modeled to understand its dynamical impact. A series of studies have progressively refined this modeling framework [12–14]. These works not only establish the stability of the proposed models but also confirm through numerical simulations, that CTLs reduce viral load and infected cell counts by eliminating infected cells, while increasing the population of uninfected CD4+ T cells. For example, Elaiw and Alshamrani [13] established a foundational model that demonstrated that a strong CTL response can clear infections, provided the immune activation rate exceeds a critical threshold, while also and highlighted the potential destabilizing effect of silent cell-to-cell spread. Ren et al. [14] introduced intracellular delays and saturated immune responses, thereby showing that these biological realities can induce rich dynamics, including stability switches and Hopf bifurcations, thus emphasizing the nonlinear and time-lagged nature of CTL-mediated control. Sutimin et al. [15] developed a mathematical model incorporating cell-to-cell transmission of HIV-1 and CTL immune

response to evaluate and compare the efficacy of RTI and PI combination therapies, finding RTI to be more effective in reducing infection. These models underscore the pivotal regulatory role of CTLs in suppressing HIV replication, primarily through the direct elimination of virus-producing cells, which forms the biological rationale for incorporating CTL dynamics in our current framework.

Our study extends the ordinary differential equation (ODE) system from [5] to incorporate the CTL immune response, thus investigating a more biologically realistic scenario of HIV transmission dynamics. Following the analytical frameworks established in prior studies [16–18], we systematically examine the existence and local stability of all system equilibria. To identify the key parameters which govern the system's behavior, we perform a global sensitivity analysis on both the basic reproduction number and the immune response reproduction number using the Latin Hypercube Sampling-Partial Rank Correlation Coefficient (LHS-PRCC) method [19, 20]. Furthermore, we investigate how these critical parameters vary with different levels of drug efficacy. This work provides theoretical insights to understand HIV persistence and to optimize therapeutic strategies.

This paper is structured as follows: in Section 2, we develop an HIV dynamics model that incorporates antiretroviral therapy, CTL immune response, and two types of infected cells; in Section 3, we prove the positivity and boundedness of the solutions and define the basic and immune reproduction numbers; in Section 4, we analyze the stability of the infection-free equilibrium, the infected but immune-free equilibrium, and the infected equilibrium with immunity under different threshold conditions; in Section 5, we provide numerical simulations to illustrate the dynamical behaviors; in Section 6, we use the LHS-PRCC method to identify key parameters that influence the reproduction numbers and examine the impact of drug efficacy on the dynamics; and finally, in Section 7, we present the discussion and conclusions.

2. Model formulation

To mechanistically capture the dynamics of HIV infection, it is essential to recognize that infected cells can be partitioned into distinct virological states: the pre-reverse transcription (Pre-RT) and post-reverse transcription (Post-RT) stages [21]. This distinction is fundamental because reverse transcription represents a rate-limiting step in the viral life cycle. Zack et al. [22] provided the direct experimental evidence for the Pre-RT stage, thereby showing that incomplete reverse transcripts in quiescent cells constitute a labile, pre-integration intermediate which can be reactivated to complete reverse transcription (transitioning to a Post-RT-like state) upon cellular activation. The intracellular virological distinction has direct implications for immune recognition. The stage of viral replication likely determines the surface antigen presentation of infected cells, thereby influencing their susceptibility to CTL-mediated killing [12–14]. To capture this interplay between intracellular viral progression and the host immune response, and building upon the modeling frameworks established in references [5, 18], we formulate an HIV model that incorporates reverse transcriptase inhibitors (RTIs) and two subclasses of infected $CD4^+$ T cells:

$$\begin{cases} \dfrac{dT}{dt} = \lambda - dT(t) - kT(t)V(t) - \beta T(t)I_2(t) + (\alpha + \eta\phi)I_1(t), \\ \dfrac{dI_1}{dt} = kT(t)V(t) + \beta T(t)I_2(t) - (\alpha + \phi + \sigma_1)I_1(t), \\ \dfrac{dI_2}{dt} = (1-\eta)\phi I_1(t) - \sigma I_2(t) - pI_2(t)Z(t), \\ \dfrac{dV}{dt} = N\sigma I_2(t) - cV(t), \\ \dfrac{dZ}{dt} = qI_2(t)Z(t) - bZ(t). \end{cases} \tag{2.1}$$

Here, $T(t)$ represents the concentration of uninfected CD4$^+$ T cells at time t. Infected CD4$^+$ T cells are divided into two subclasses, namely $I_1(t)$ and $I_2(t)$, which are the concentrations of Pre-RT infected cells and the concentration of infected CD4$^+$ T cells of the Post-RT subclass at time t, respectively. $V(t)$ stands for the viral load at time t. $Z(t)$ represents the concentration of CTLs at time t. The parameter inequality $d < \sigma_1$ indicates that infected cells have a higher mortality rate compared to healthy cells; this is because extensive HIV replication and assembly within infected cells disrupts normal cellular structures and functions, which leads to accelerated apoptosis [23]. The parameters used in model (2.1) and their biological interpretations are summarized in Table 1.

Table 1. Parameters used in model (2.1).

Parameter	Definition
λ	Recruitment rate of uninfected T cells
d	Death rate of uninfected T cells
k	Virus-to-cell infection rate
β	Cell-to-cell infection rate
α	Reverting rate of Pre-RT infected cells return to uninfected cells
η	Dosage of the reverse transcriptase inhibitor (drug efficacy)
ϕ	Transition rate from Pre-RT infected cells to post-RT infected cells
σ	Death rate of infected cells
σ_1	Death rate of Pre-RT infected cells
p	Rate of CTL-mediated clearance of post-RT infected cells
N	Total number of viral particles produced by an infected cell
c	Clearance rate of viruses
q	Production rate of CTLs by productively infected cells
b	Death rate of CTL immune cells

3. Preliminary results

In this section, we first investigate the positivity and boundedness of solutions of model (2.1).

3.1. Positivity and boundedness of solutions

Based on the actual characteristics of the HIV viruses, we assume the following initial conditions for model (2.1):

$$T(0) > 0, \quad I_1(0) > 0, \quad I_2(0) > 0, \quad V(0) > 0, \quad Z(0) > 0. \tag{3.1}$$

Theorem 3.1. *Any solution of* (2.1) *that satisfies* (3.1) *is positive.*

Proof. Let $(T(t), I_1(t), I_2(t), V(t), Z(t))$ be any solution of (2.1). By way of contradiction, suppose at least one of the component is not positive. Let

$$W(t) = \min\{T(t), I_1(t), I_2(t), V(t), Z(t)\}.$$

Then, as $W(0) > 0$, there exists $t_1 > 0$ such that $W(t_1) = 0$ and $W(t) > 0$ for $0 \leq t < t_1$. We claim that $I_1(t_1) = 0$. Otherwise, $I_1(t) > 0$ for $t \in [0, t_1]$. This combined with the first and the third equations of (2.1), gives $T(t) > 0$ and $I_2(t) > 0$ for $t \in [0, t_1]$, respectively. Then, using $I_2(t) > 0$ for $t \in [0, t_1]$ and the fourth equation of (2.1), we get $V(t) > 0$ for $t \in [0, t_1]$. Clearly, $Z(t) > 0$ for $t > 0$ from the fifth equation of (2.1). Thus $W(t_1) > 0$, a contradiction to the choice of t_1. This proves the claim. However, it follows from $T(t) \geq 0, I_2(t) \geq 0$, and $V(t) \geq 0$ for $t \in [0, t_1]$, that we can get $I_1(t) > 0$ for $t \in [0, t_1]$ from the second equation of (2.1), which is a contradiction to $I_1(t_1) = 0$. This completes to the proof.

The follow result shows that the solution of model (2.1) with (3.1) remains ultimately bounded.

Theorem 3.2. *Solutions of model* (2.1) *that satisfy the initial conditions* (3.1) *are ultimately uniformly bounded.*

Proof. Let $(T(t), I_1(t), I_2(t), V(t), Z(t))$ be any solution. Define the following:

$$H(t) = T(t) + I_1(t) + I_2(t) + \frac{p}{q}Z(t).$$

Differentiating $H(t)$ yields the following:

$$\frac{dH(t)}{dt} = \lambda - \left(dT(t) + \sigma_1 I_1(t) + \sigma I_2(t) + \frac{bp}{q}Z(t)\right) \leq \lambda - MH(t),$$

where $M = \min\{d, \sigma, \sigma_1, b\}$. Then, we have $\limsup_{t\to\infty} H(t) \leq \frac{\lambda}{M}$. Therefore, for any sufficiently small $\varepsilon \geq 0$, there exists $t_2 > 0$ such that $H(t) \leq \frac{\lambda}{M} + \varepsilon$ for $t \geq t_2$. Then, for $t \geq t_2$, $\frac{dV(t)}{dt} \leq N\sigma(\frac{\lambda}{M} + \varepsilon) - cV(t)$, which implies $\limsup_{t\to\infty} V(t) \leq \frac{N\sigma(\frac{\lambda}{M}+\varepsilon)}{c}$. Since$\varepsilon$ is arbitrary, $\limsup_{t\to\infty} V(t) \leq \frac{N\sigma\lambda}{cM}$. This completes the proof.

From the proof of Theorem 3.2, we can easily see that the set

$$\Omega = \left\{(T(t), I_1(t), I_2(t), V(t), Z(t)) \in \mathbb{R}^5_{+0} : T(t) + I_1(t) + I_2(t) + Z(t) \leq \frac{\lambda}{M} \text{ and } V(t) \leq \frac{N\delta\lambda}{cM}\right\},$$

where

$$\mathbb{R}^5_{+0} = \{(T(t), I_1(t), I_2(t), V(t), Z(t)) \in \mathbb{R}^5 | T(t) > 0, I_1(t) > 0, I_2(t) > 0, Z(t) > 0\}$$

is a positively invariant set for model (2.1).

3.2. The basic reproductive number and equilibria

Clearly, model (2.1) always admits a disease-free equilibrium $E^0 = (T^0, I_1^0, I_2^0, V^0, Z^0) = (\frac{\lambda}{d}, 0, 0, 0, 0)$. With the next generation matrix method, the matrices for the new infection terms $\mathbb{F}$ and transition terms $\mathbb{V}$ are as follows:

$$\mathbb{F} = \begin{pmatrix} 0 & \beta T^0 & kT^0 \\ 0 & 0 & 0 \\ 0 & 0 & 0 \end{pmatrix}, \quad \mathbb{V} = \begin{pmatrix} \alpha + \phi + \sigma_1 & 0 & 0 \\ -(1-\eta)\phi & \sigma + pZ^0 & 0 \\ 0 & -N\sigma & c \end{pmatrix},$$

respectively. Here, the matrix $\mathbb{V}$ encompasses all transitions out of the infected compartments (Pre-RT and Post-RT cells), including natural death, immune-mediated clearance, and progression between stages. Its diagonal entries represent the total removal rates (e.g., through natural death or immune clearance) from the corresponding compartment. The off-diagonal entries represent transitions into a compartment from another infected state. For instance, in our model, the term $(1-\eta)\phi$ appears as an off-diagonal entry that denotes the progression from Pre-RT cells (I_1) to the Post-RT cells (I_2), while $N\sigma$ represents the production of virus from the Post-RT cells (I_2).

The basic reproduction number R_0 of model (2.1) is given by the following:

$$\begin{aligned} R_0 &= \rho(\mathbb{F}\mathbb{V}^{-1}) \\ &= \frac{\beta T^0 c\phi(1-\eta) + \sigma N T^0 k\phi(1-\eta)}{c\sigma(\alpha+\phi+\sigma_1)} \\ &= \frac{\lambda\phi(1-\eta)(\beta c + \sigma N k)}{dc\sigma(\alpha+\phi+\sigma_1)}. \end{aligned}$$

The derived basic reproduction number can be biologically interpreted as follows:

$$R_0 = \underbrace{\frac{\lambda}{d}}_{(I)} \times \underbrace{\frac{\phi(1-\eta)}{\alpha+\phi+\sigma_1}}_{(II)} \times \underbrace{\left(\frac{\beta c + \sigma N k}{c\sigma}\right)}_{(III)}.$$

Term (I): $\frac{\lambda}{d}$ is the steady-state number of susceptible target cells (T^0) in the absence of infection, thus representing the pool of cells available for the virus to infect.

Term (II): $\frac{\phi(1-\eta)}{\alpha+\phi+\sigma_1}$ is the probability that a newly infected cell enters the chronically infected state (I_2) rather than being cleared by the immune system or dying naturally. Here, $(1-\eta)$ quantifies the reduction in cell-to-cell transmission due to partial inhibition.

Term (III): $\frac{\beta c+\sigma N k}{c\sigma} = \frac{\beta}{\sigma} + \frac{Nk}{c}$ combines two distinct infection pathways:
$\frac{\beta}{\sigma}$ denotes the number of new susceptible cells infected via cell-to-cell transmission per chronically infected cell, where β is the infection rate, and $\frac{1}{\sigma}$ is the average lifespan of a chronically infected cell. $\frac{Nk}{c}$ denotes the number of new susceptible cells infected per virion, where k is the cell-to-cell transmission rate, N is the burst size, and $\frac{1}{c}$ is the average lifespan of a free virion.

Thus, $R_0 > 1$ represents the expected number of secondary chronically infected cells (I_2) produced by a single chronically infected cell introduced into a fully susceptible target cell population, thus accounting for both free-virus and cell-to-cell transmission modes under partial inhibition.

In addition to the equilibrium E_0, when $R_0 > 1$, model (2.1) also admits an infected but immune-free equilibrium $\overline{E} = (\overline{T}, \overline{I_1}, \overline{I_2}, \overline{V}, \overline{Z})$, where $\overline{Z} = 0$, and $\overline{T}$, $\overline{I_1}$, $\overline{I_2}$, $\overline{V}$ are given by the following:

$$\overline{T} = \frac{c\sigma(\alpha+\phi+\sigma_1)}{\phi(1-\eta)(\beta c+\sigma N k)} = \frac{T^0}{R_0}, \overline{I_1} = \frac{\lambda\left(1-\frac{1}{R_0}\right)}{\sigma_1+\phi(1-\eta)}, \overline{I_2} = \frac{\phi(1-\eta)\overline{I_1}}{\sigma}, \overline{V} = \frac{N\phi(1-\eta)\overline{I_1}}{c}.$$

According to [16], we define the CTL immune response reproduction number R_1 for model (2.1) as follows:

$$R_1 = \frac{q}{b}\overline{I_2} = \frac{q\lambda\phi\left(1-\frac{1}{R_0}\right)(1-\eta)}{b\sigma(\sigma_1+\phi(1-\eta))}.$$

Note that $q\overline{I_2}$ represents the number of newly activated and differentiated CTL cells per unit time through viral antigen present in the absence of CTL immune response, and $\frac{1}{b}$ is the average survival time of CTL cells. Multiplying these two quantities gives the expected number of cytotoxic T lymphocytes produced by one CTL cell during its lifetime, stimulated by cells in the effectively infected state.

When $R_1 > 1$, there exists a unique infected equilibrium with immunity $E^* = (T^*, I_1^*, I_2^*, V^*, Z^*)$, where

$$I_2^* = \frac{b}{q}, V^* = \frac{Nb\sigma}{cq}, I_1^* = \frac{b(\sigma+pZ^*)}{q\phi(1-\eta)}, T^* = \frac{c(\alpha+\phi+\sigma_1)(\sigma+pZ^*)}{\phi(1-\eta)(\beta c+\sigma N k)},$$

and

$$Z^* = \frac{\sigma}{p}\cdot\frac{1}{\lambda\phi(1-\eta)+bR_0\sigma(\sigma_1+\phi(1-\eta))}\cdot\frac{1}{bR_0\sigma(\sigma_1+\phi(1-\eta))}\cdot(R_1-1).$$

In the next section, we conduct a detailed stability analysis of these equilibria and present the local stability conditions for each.

4. Stability of the equilibria E^0, $\overline{E}$, and E^*

In this section, we study the local and global stability of three equilibria: The infection-free equilibrium, the infected but immune-free equilibrium, and the infected equilibrium with immunity.

Let $\hat{E} = (\hat{T}, \hat{I}_1, \hat{I}_2, \hat{V}, \hat{Z})$ be an equilibrium of (2.1). Then, the Jacobian matrix at $\hat{E}$ is as follows:

$$J(\hat{E}) = \begin{pmatrix} -d-k\hat{V}-\beta\hat{I}_2 & \alpha+\eta\phi & -\beta\hat{T} & -k\hat{T} & 0 \\ k\hat{V}+\beta\hat{I}_2 & -(\alpha+\phi+\sigma_1) & \beta\hat{T} & k\hat{T} & 0 \\ 0 & (1-\eta)\phi & -\sigma-p\hat{Z} & 0 & -p\hat{I}_2 \\ 0 & 0 & N\sigma & -c & 0 \\ 0 & 0 & q\hat{Z} & 0 & q\hat{I}_2-b \end{pmatrix}.$$

Theorem 4.1. *When $R_0 < 1$, the infection-free equilibrium E^0 of model* (2.1) *is locally asymptotically stable; alternatively, it is unstable if $R_0 > 1$.*

Proof. The characteristic equation of $J(E^0)$ is as follows:

$$\Delta_{E^0}(S) = (S+d)(S+b)q_1(S) = 0,$$

where

$$q_1(S) = (S + \alpha + \phi + \sigma_1)(S + \sigma)(S + c) - (1 - \eta)\phi T^0[\beta(S + c) + N\sigma k].$$

Besides the eigenvalues $S_1 = -d$ and $S_2 = -b$, the others are determined by $q_1(S) = 0$. If $R_0 > 1$, then $q_1(0) = (\alpha + \phi + \sigma_1)\sigma c(1 - R_0) < 0$. Note that $\lim_{S\to\infty} q_1(S) = \infty$. Then, $q_1(S) = 0$ has a positive root, hence E^0 is unstable. Now, assuming $R_0 < 1$, we claim that all roots of $q_1(S) = 0$ have negative real parts. Otherwise, let S^* be one root of $q_1(S) = 0$ with $Re(S^*) \geq 0$. Then, we have the following:

$$\begin{aligned} 1 &= \left| \frac{(1 - \eta)\phi\beta T^0}{(S^* + \alpha + \phi + \sigma_1)(S^* + \sigma)} + \frac{(1 - \eta)\phi k T^0 N\sigma}{(S^* + \alpha + \phi + \sigma_1)(S^* + \sigma)(S^* + c)} \right| \\ &\leq \left| \frac{(1 - \eta)\phi\beta T^0}{(S^* + \alpha + \phi + \sigma_1)(S^* + \sigma)} \right| + \left| \frac{(1 - \eta)\phi k T^0 N\sigma}{(S^* + \alpha + \phi + \sigma_1)(S^* + \sigma)(S^* + c)} \right| \\ &\leq \frac{(1 - \eta)\phi T^0\beta}{\sigma(\alpha + \phi + \sigma_1)} + \frac{(1 - \eta)\phi T^0 Nk}{c(\alpha + \phi + \sigma_1)} = R_0. \end{aligned}$$

This leads to a contradiction. Therefore, when $R_0 < 1$, E^0 is locally asymptotically stable.

In fact, the local stability of E_0 implies its global stability.

Lemma 4.1. (Fluctuation lemma [24]) Let $f : (t_0, \infty) \to \mathbb{R}$ be bounded and continuously differentiable. Then, there exist sequences $t_n, s_n \to \infty$ with the following properties:

$$f(t_n) \to f^\infty, \quad f'(t_n) \to 0, \quad f(s_n) \to f_\infty, \quad f'(s_n) \to 0 \quad \text{as } n \to \infty,$$

where

$$f^\infty = \limsup_{t\to\infty} f(t) \quad \text{and} \quad f_\infty = \liminf_{t\to\infty} f(t).$$

Theorem 4.2. *If $R_0 < 1$, then the infection-free equilibrium E_0 of model (2.1) is globally asymptotically stable.*

Proof. By Lemma 4.1, it suffices to show that E_0 is globally attractive. Let $(T(t), I_1(t), I_2(t), V(t), Z(t))$ be any solution of model (2.1). Then, it is bounded and continuously differentiable on $(0, \infty)$.

Let t_n be a sequence with $t_n \to \infty$ such that $V(t_n) \to V^\infty$ and $V'(t_n) \to 0$ as $n \to \infty$. Then, by the fourth equation of (2.1), we have the following:

$$\frac{dV(t_n)}{dt} = N\sigma I_2(t_n) - cV(t_n).$$

Letting $n \to \infty$ gives either

$$0 \leq N\sigma I_2^\infty - cV^\infty$$

or

$$V^\infty \leq \frac{N\sigma}{c} I_2^\infty.$$

Similarly, from the third equation, we get the following:

$$I_2^\infty \leq \frac{(1-\eta)\phi}{\sigma} I_1^\infty.$$

Define $L(t) = T(t) + I_1(t)$. We have the following:

$$\frac{dL}{dt} = \lambda - dT(t) - [(1-\eta)\phi + \sigma_1]I_1(t).$$

Since $d < \sigma_1$,

$$\frac{dL}{dt} \leq \lambda - d(T(t) + I_1(t)) = \lambda - dL(t).$$

We have $\limsup_{t\to\infty}(T(t) + I_1(t)) \leq \frac{\lambda}{d}$, which implies $T^\infty \leq \frac{\lambda}{d}$.

Now, let s_n be a sequence with $s_n \to \infty$ such that $I_1(s_n) \to I_1^\infty$ and $I_1'(s_n) \to 0$ as $n \to \infty$. Evaluating the second equation of (2.1) at s_n and letting $n \to \infty$ gives the following:

$$0 \leq kT^\infty V^\infty + \beta T^\infty I_2^\infty - (\alpha + \phi + \sigma_1)I_1^\infty.$$

This, together with $V^\infty \leq \frac{N\sigma}{c} I_2^\infty$, $T^\infty \leq \frac{\lambda}{d}$, and $I_2^\infty \leq \frac{(1-\eta)\phi}{\sigma} I_1^\infty$, implies that

$$\begin{aligned} 0 &\leq \frac{kN\sigma}{c} I_2^\infty T^\infty + \beta I_2^\infty T^\infty - (\alpha + \phi + \sigma_1)I_1^\infty \\ &\leq \frac{(1-\eta)\phi}{\sigma}\left(\frac{kN\sigma}{c} + \beta\right)T^\infty I_1^\infty - (\alpha + \phi + \sigma_1)I_1^\infty \\ &\leq (\alpha + \phi + \sigma_1)(R_0 - 1)I_1^\infty. \end{aligned}$$

By $R_0 < 1$, we get $I_1^\infty = 0$. Then, from $I_2^\infty \leq \frac{(1-\eta)\phi}{\sigma} I_1^\infty$, we have $I_2^\infty = 0$. From $\frac{dZ(t)}{dt} = qI_2(t)Z(t) - bZ(t)$, we have $Z^\infty = 0$. To sum up, we have shown $I_1^\infty = I_2^\infty = V^\infty = Z^\infty = 0$; hence,

$$\lim_{t\to\infty} I_1(t) = \lim_{t\to\infty} I_2(t) = \lim_{t\to\infty} V(t) = \lim_{t\to\infty} Z(t) = 0. \tag{4.1}$$

To finish the proof, we show that $\lim_{t\to\infty} T(t) = \frac{\lambda}{d}$. This is done by showing $T_\infty \geq \frac{\lambda}{d}$ as $T^\infty \leq \frac{\lambda}{d}$. In fact, let u_n be a sequence such that $u_n \to \infty$, $T(u_n) \to T_\infty$, and $T'(u_n) \to 0$ as $n \to \infty$. Then, from the first equation of (2.1) obtain the following:

$$\frac{dT(u_n)}{dt} = \lambda - dT(u_n) - kT(u_n)V(u_n) - \beta T(u_n)I_2(u_n) + (\alpha + \eta\phi)I_1(u_n).$$

Letting $n \to \infty$, with the help of (4.1), we get $T_\infty = \frac{\lambda}{d}$. This completes the proof.

Theorem 4.3. *When $R_0 > 1$ and $R_1 < 1$, the infect but immune-free equilibrium $\overline{E}$ of model* (2.1) *is locally asymptotically stable.*

Proof. The characteristic equation at the equilibrium $\overline{E}$ is as follows:

$$\Delta_{\overline{E}}(S) = (S + b - q\bar{I}_2)q_2(S) = 0,$$

where

$$\begin{aligned} q_2(S) &= (S+d)(S+\alpha+\phi+\sigma_1)(S+\sigma)(S+c) \\ &\quad + (S+\sigma)(S+c)[S+(1-\eta)\phi+\sigma_1](k\overline{V}+\beta\bar{I}_2) \\ &\quad - (S+d)(1-\eta)\phi[\beta\overline{T}(S+c)+\overline{T}Nk\sigma]. \end{aligned}$$

From $S+b-q\bar{I}_2=0$, we obtain $S=b(R_1-1)$, which is negative as $R_1<1$. Our goal is to prove that all the other eigenvalues determined by $q_2(S)=0$ have negative real parts. By way of contradiction. Suppose S is a root with a non-negative real part. Then, we have $q_2(S)=0$ or equivalently

$$\begin{aligned} &\left|1+\frac{[S+(1-\eta)\phi+\sigma_1](k\overline{V}+\beta\bar{I}_2)}{(S+\alpha+\phi+\sigma_1)(S+d)}\right| = \left|\frac{(1-\eta)\phi[\beta\overline{T}(S+c)+\overline{T}Nk\sigma]}{(S+\alpha+\phi+\sigma_1)(S+\sigma)(S+c)}\right| \\ &< \left|\overline{T}\right|\cdot\frac{R_0}{T^0}=1. \end{aligned}$$

Define $F_1=\left|1+\frac{(S+(1-\eta)\phi+\sigma_1)(k\overline{V}+\beta\bar{I}_2)}{(S+\alpha+\phi+\sigma_1)(S+d)}\right|$. Assume $S=x+yi$, where x is the real part and y is the imaginary part of the eigenvalue. Substituting it into F_1 gives the following:

$$\begin{aligned} F_1 &= \left|1+\frac{[x+yi+(1-\eta)\phi+\sigma_1](k\overline{V}+\beta\bar{I}_2)}{(x+yi+\alpha+\phi+\sigma_1)(x+yi+d)}\right| \\ &= \left|1+\frac{[x+yi+(1-\eta)\phi+\sigma_1](k\overline{V}+\beta\bar{I}_2)}{[(x+\alpha+\phi+\sigma_1)(x+d)-y^2]+yi\cdot(2x+\alpha+\phi+\sigma_1+d)}\right|. \end{aligned} \tag{4.2}$$

Set $A=(x+\alpha+\phi+\sigma_1)(x+d)-y^2$, $B=2x+\alpha+\phi+\sigma_1+d$, and rationalize the denominator of the fraction in (4.2) to obtain the following:

$$\begin{aligned} F_1 &= \left|1+\frac{[x+yi+(1-\eta)\phi+\sigma_1](k\overline{V}+\beta\bar{I}_2)}{A+yiB}\right| \\ &= \left|1+\frac{[x+yi+(1-\eta)\phi+\sigma_1](k\overline{V}+\beta\bar{I}_2)(A-yiB)}{(A+yiB)(A-yiB)}\right| \\ &= \left|1+\frac{[x+yi+(1-\eta)\phi+\sigma_1](k\overline{V}+\beta\bar{I}_2)(A-yiB)}{A^2+B^2y^2}\right| \\ &= |1+W_1+W_2i|, \end{aligned}$$

where

$$\begin{aligned} W_1 &= \frac{y^2(x+\alpha+\eta\phi+d)(k\overline{V}+\beta\bar{I}_2)+[x+(1-\eta)\phi+\sigma_1](k\overline{V}+\beta\bar{I}_2)(x+\alpha+\phi+\sigma_1)(x+d)}{A^2+B^2y^2}, \\ W_2 &= \frac{y(k\overline{V}+\beta\bar{I}_2)[(x+\alpha+\phi+\sigma_1)(x+d)-y^2]}{A^2+B^2y^2} \\ &\quad - \frac{y(k\overline{V}+\beta\bar{I}_2)(2x+\alpha+\phi+\sigma_1+d)[x+(1-\eta)\phi+\sigma_1]}{A^2+B^2y^2}. \end{aligned}$$

As $x\geq 0$, we know $W_1>0$. It follows that

$$F_1=|1+W_1+W_2\cdot i|=\sqrt{(1+W_1)^2+W_2^2}>1,$$

which is a contradiction to the assumption that $F_1 < 1$. Therefore, when $R_0 > 1$ and $R_1 < 1$, $\overline{E}$ is locally asymptotically stable.

Now, we consider the local asymptotical stability of E^*. The characteristics equation at E^* is given by

$$\Delta_{E^*}(S) = S^5 + a_1S^4 + a_2S^3 + a_3S^2 + a_4S + a_5,$$

with the relations

$$I_2^*q = b, \quad T^* = \frac{c(\alpha+\phi+\sigma_1)(\sigma+pZ^*)}{\phi(1-\eta)(\sigma Nk+\beta c)}, \quad \frac{\beta c(\alpha+\phi+\sigma_1)(\sigma+pZ^*)}{(\sigma Nk+\beta c)} < (\alpha+\phi+\sigma_1)(\sigma+pZ^*).$$

We obtain the following:

$$a_1 = \sigma_1+\sigma+\alpha+c+d+\phi+kV^*+pZ^*+\beta I_2^* > 0,$$

$$\begin{aligned}
a_2 &= \alpha d + cd + c\phi + d\phi + \alpha\sigma + c\sigma + c\sigma_1 + d\sigma + d\sigma_1 + \phi\sigma + \sigma\sigma_1 + \alpha c + I_2^*Nk\sigma + I_2^*Z^*\beta p \\
&\quad + I_2^*\beta c + I_2^*\beta\phi(1-\eta) + I_2^*\beta\sigma + I_2^*\beta\sigma_1 + Z^*\alpha p + Z^*bp + Z^*cp + Z^*dp + Z^*p\phi + Z^*p\sigma_1 \\
&\quad + \frac{I_2^*Nk\sigma^2}{c} + \frac{I_2^*NZ^*kp\sigma}{c} + \frac{I_2^*Nk\sigma\sigma_1}{c} + \frac{I_2^*Nk\phi\sigma}{c}(1-\eta) - \frac{\beta c(\sigma+Z^*p)(\alpha+\phi+\sigma_1)}{(\beta c+Nk\sigma)} \\
&> \alpha d + cd + c\phi + d\phi + c\sigma + c\sigma_1 + d\sigma + d\sigma_1 + \alpha c + I_2^*Nk\sigma \\
&\quad + I_2^*\beta c + I_2^*\beta\phi(1-\eta) + I_2^*\beta\sigma + I_2^*\beta\sigma_1 + Z^*bp + Z^*cp + I_2^*Z^*\beta p \\
&\quad + Z^*dp + \frac{I_2^*Nk\sigma^2}{c} + \frac{I_2^*NZ^*kp\sigma}{c} + \frac{I_2^*Nk\sigma\sigma_1}{c} + \frac{I_2^*Nk\phi\sigma}{c}(1-\eta) > 0,
\end{aligned}$$

$$\begin{aligned}
a_3 &= cd\phi + \alpha c\sigma + \alpha d\sigma + cd\sigma + cd\sigma_1 + c\phi\sigma + d\phi\sigma + c\sigma\sigma_1 + d\sigma\sigma_1 + I_2^*NZ^*kp\sigma + Z^*bp\sigma_1 \\
&\quad + Z^*cp\sigma_1 + Z^*dp\sigma_1 + I_2^*Nk\sigma^2 + I_2^*\beta c\phi(1-\eta) + I_2^*\beta c\sigma + I_2^*\beta c\sigma_1 + Z^*\alpha bp + Z^*\alpha cp \\
&\quad + I_2^*\beta\phi\sigma(1-\eta) + Z^*bcp + Z^*\alpha dp + Z^*bdp + Z^*cdp + I_2^*\beta\sigma\sigma_1 + Z^*bp\phi + Z^*cp\phi + Z^*dp\phi \\
&\quad + I_2^*Z^*b\beta p + I_2^*Z^*\beta cp + \alpha cd + I_2^*Nk\phi\sigma(1-\eta) + I_2^*Z^*\beta p\phi(1-\eta) + I_2^*Nk\sigma\sigma_1 + I_2^*Z^*\beta p\sigma_1 \\
&\quad + \frac{I_2^*Nk\phi\sigma^2}{c}(1-\eta) + \frac{I_2^*Nk\sigma^2\sigma_1}{c} + \frac{I_2^*NZ^*kp\phi\sigma}{c}(1-\eta) + \frac{I_2^*NZ^*kp\sigma\sigma_1}{c} + \frac{I_2^*NZ^*bkp\sigma}{c} \\
&\quad - c(\sigma+Z^*p)(\alpha+\phi+\sigma_1) - \frac{\beta cd(\sigma+Z^*p)(\alpha+\ phi+\sigma_1)}{\beta c+Nk\sigma} \\
&> Z^*\alpha bp + I_2^*Nk\sigma^2 + I_2^*\beta c\phi(1-\eta) + I_2^*\beta c\sigma + I_2^*\beta c\sigma_1 + cd\sigma + cd\sigma_1 + I_2^*Z^*\beta p\sigma_1 \\
&\quad + I_2^*\beta\phi\sigma(1-\eta) + Z^*bcp + Z^*bdp + Z^*cdp + I_2^*\beta\sigma\sigma_1 + Z^*bp\phi + Z^*bp\sigma_1 + cd\phi \\
&\quad + I_2^*Z^*b\beta p + I_2^*Z^*\beta cp + \alpha cd + I_2^*Nk\phi\sigma(1-\eta) + I_2^*Z^*\beta p\phi(1-\eta) + I_2^*Nk\sigma\sigma_1 + I_2^*NZ^*kp\sigma \\
&\quad + \frac{I_2^*Nk\phi\sigma^2}{c}(1-\eta) + \frac{I_2^*Nk\sigma^2\sigma_1}{c} + \frac{I_2^*NZ^*kp\phi\sigma}{c}(1-\eta) + \frac{I_2^*NZ^*kp\sigma\sigma_1}{c} + \frac{I_2^*NZ^*bkp\sigma}{c} > 0,
\end{aligned}$$

$$\begin{aligned}
a_4 &= Z^*\alpha bcp + I_2^*\beta c\sigma\sigma_1 + Z^*bcp\phi + Z^*bcp\sigma_1 + Z^*bcdp + I_2^*\beta c\phi\sigma(1-\eta) \\
&\quad + I_2^*Nk\phi\sigma^2(1-\eta) + I_2^*Z^*\beta cp\phi(1-\eta) + I_2^*Nk\sigma^2\sigma_1 + I_2^*Z^*\beta cp\sigma_1 + Z^*\alpha bdp \\
&\quad + I_2^*Z^*b\beta cp + I_2^*Z^*b\beta p\sigma_1 + I_2^*Z^*b\beta p\phi(1-\eta) + I_2^*NZ^*bkp\sigma + Z^*bdp\sigma_1 + Z^*bdp\phi \\
&\quad + \frac{I_2^*NZ^*bkp\phi\sigma}{c}(1-\eta) + I_2^*NZ^*kp\phi\sigma(1-\eta) + \frac{I_2^*NZ^*bkp\sigma\sigma_1}{c} + I_2^*NZ^*kp\sigma\sigma_1 > 0,
\end{aligned}$$

and

$$a_5 = Z^* bp[\alpha cd + cd\phi + cd\sigma_1 + I_2^*\beta c\phi(1-\eta) + I_2^*\beta c\sigma_1 + I_2^* Nk\phi\sigma(1-\eta) + I_2^* Nk\sigma\sigma_1] > 0.$$

Applying the Routh-Hurwitz criterion [25], it follows that all roots of $\Delta_{E^*}(S) = 0$ have negative real parts if and only if $H_i > 0$ $(i = 1, 2, 3, 4, 5)$:

$$\begin{aligned}
&H_1 = a_1 > 0,\\
&H_2 = a_1 a_2 - a_3 > 0,\\
&H_3 = \begin{vmatrix} a_1 & a_3 & a_5 \\ 1 & a_2 & a_4 \\ 0 & a_1 & a_3 \end{vmatrix} = a_3 H_2 - a_1(a_1 a_4 - a_5) > 0,\\
&H_4 = \begin{vmatrix} a_1 & a_3 & a_5 & 0 \\ 1 & a_2 & a_4 & 0 \\ 0 & a_1 & a_3 & a_5 \\ 0 & 1 & a_2 & a_4 \end{vmatrix} = a_4 H_3 - a_2 a_5 H_2 + a_5(a_1 a_4 - a_5) > 0,\\
&H_5 = \begin{vmatrix} a_1 & a_3 & a_5 & 0 & 0 \\ 1 & a_2 & a_4 & 0 & 0 \\ 0 & a_1 & a_3 & a_5 & 0 \\ 0 & 1 & a_2 & a_4 & 0 \\ 0 & 0 & a_1 & a_3 & a_5 \end{vmatrix} = a_5 H_4 > 0.
\end{aligned} \tag{4.3}$$

Then, we can obtain the following theorem:

Theorem 4.4. *If $R_1 > 1$ and condition* (4.3) *holds, then the infected equilibrium with immunity E^* of model* (2.1) *is locally asymptotically stable.*

5. Numerical results

In this section, we perform numerical simulations to quantitatively study the dynamics of model (2.1). The initial condition is given by $IC = (T(0), I_1(0), I_2(0), V(0), Z(0))$. We consider three different initial conditions: $IC_1 = (1200, 50, 25, 1, 0.1)$, $IC_2 = (800, 100, 65, 200, 1)$, and $IC_3 = (400, 200, 110, 1000, 0.5)$, which represent different stages of infection. The temporal trajectories of uninfected cells (T), Pre-RT infected cells (I_1), Post-RT infected cells(I_2), viral load (V), and CTL immune cells (Z) under the three scenarios are illustrated in Figures 1–3.

First, we demonstrate the stability of the infection-free equilibrium E_0 as shown in Figure 1. Using the parameter values of $\eta = 0.91$, with the remaining parameters taken from Table 2, we obtain a basic reproduction number of $R_0 = 0.78 < 1$. The simulation shows that during the early stage, the viral load exhibits a transient, low-level peak but is rapidly cleared, thus failing to establish a persistent infection. The populations of Pre-RT infected cells and Post-RT infected cells show a brief, limited increase before declining to zero. Healthy $CD4^+$ T cells experience a modest initial depletion but gradually recover and stabilize, while the CTL immune response is transiently activated due to the brief antigenic stimulus. This dynamic evolution is consistent with Theorem 4.2, which states that the infection-free equilibrium E_0 is globally asymptotically stable when $R_0 < 1$.

Table 2. The list of parameter values for the different numerical simulations.

Parameter	Value	Unit	Source
λ	10	$\text{mm}^{-3} \cdot \text{day}^{-1}$	[5]
d	0.01	day^{-1}	[5]
k	2.4×10^{-5}	$\text{mm}^{-3} \cdot \text{day}^{-1}$	[5]
β	10^{-5}	$\text{mm}^{-3} \cdot \text{day}^{-1}$	[5]
α	0.05	day^{-1}	[5]
ϕ	0.4	day^{-1}	[5]
σ_1	0.015	day^{-1}	[5]
σ	0.26	day^{-1}	[5]
p	2.4×10^{-6}	$\text{mm}^{-3} \cdot \text{day}^{-1}$	[10]
N	1000	virions $\cdot$ cell $^{-1}$	[5]
c	2.4	day^{-1}	[5]
q	1×10^{-5}	$\text{mm}^{-3} \cdot \text{day}^{-1}$	[10]
b	0.01	day^{-1}	[10]

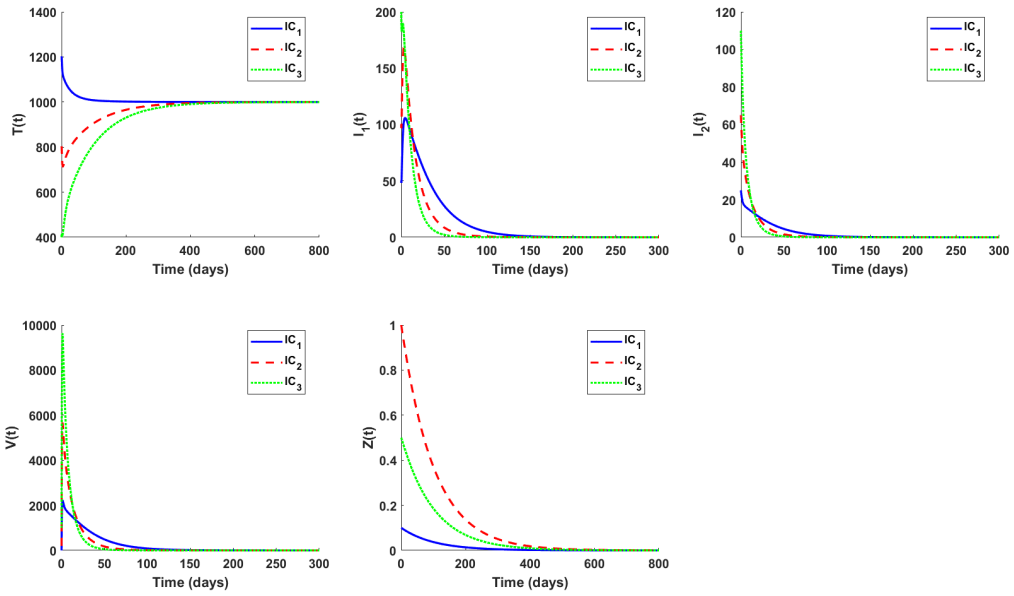

Figure 1. The infection dynamics illustrating the stability of the disease-free equilibrium E^0.

Using the parameter values $\eta = 0.35$, $N = 1500$, and $k = 3.5 \times 10^{-5}$, along with the remaining parameters from Table 2, we obtain $R_0 = 12.25 > 1$ and $R_1 = 0.03 < 1$. The time series in Figure 2 show that during the initial stage of HIV infection, the viral load V sharply increases and then stabilizes at a high level, thus indicating persistent viral replication when $R_0 > 1$. The populations of Pre-RT infected cells and Post-RT infected cells persist without declining, while the concentration of healthy CD4$^+$ T cells significantly decreases and remains at a low level. The observed convergence of all state variables to steady levels provides numerical evidence for the local asymptotic stability of the infected but immune-free equilibrium $\overline{E}$, which is in full agreement with the analytical condition $R_0 > 1$

and $R_1 < 1$ given in Theorem 4.3.

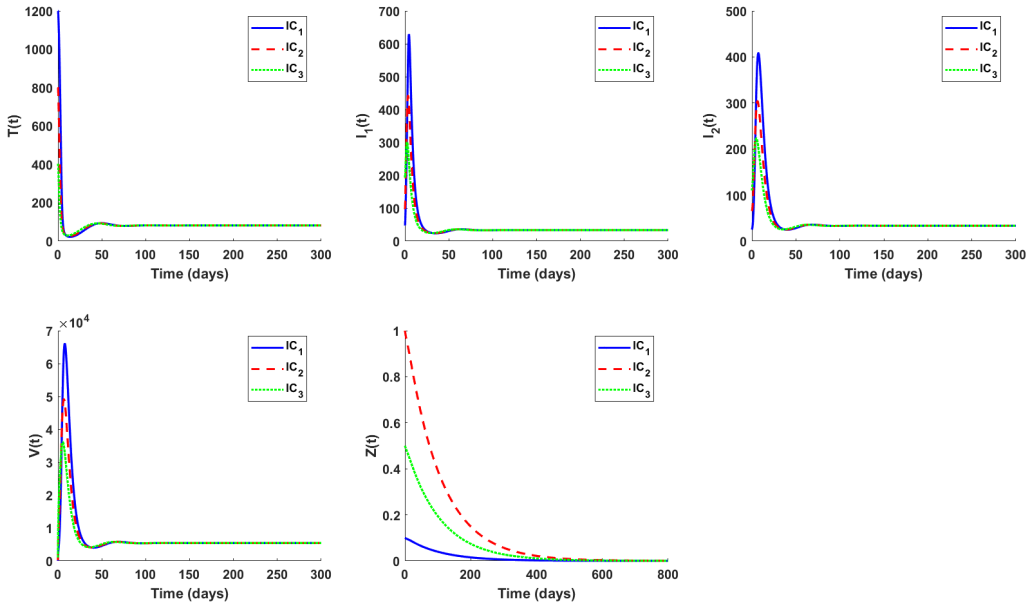

Figure 2. The infection dynamics illustrating the stability of the infected but immune-free equilibrium $\overline{E}$.

Using the parameter values $\eta = 0.4$, $q = 8\times10^{-4}$, and $b = 0.001$, and the remaining parameters from Table 2, we obtain $R_0 = 5.18 > 1$ and $R_1 = 23.37 > 1$. Following the Routh-Hurwitz stability criterion described in Theorem 4.4, and using the given parameter values, the coefficients of the characteristic polynomial are obtained as follows:

$$a_1 = 4.020924, \quad a_2 = 4.441039, \quad a_3 = 0.058312, \quad a_4 = 0.003299, \quad a_5 = 0.000012.$$

The corresponding Hurwitz determinants are calculated as follows:

$$\begin{aligned}
H_1 &= a_1 = 4.020924,\\
H_2 &= a_1a_2 - a_3 = 17.798770,\\
H_3 &= a_3H_2 - a_1(a_1a_4 - a_5) = 0.984579,\\
H_4 &= a_4H_3 - a_2a_5H_2 + a_5(a_1a_4 - a_5) = 0.002331,\\
H_5 &= a_5H_4 = 0.000000027972.
\end{aligned}$$

Clearly, all determinants H_1 through H_5 are strictly positive; therefore, the Routh-Hurwitz stability conditions are satisfied. The time series in Figure 3 show the corresponding dynamics. These simulation results confirm the local asymptotic stability of the infected equilibrium with immunity E^* when $R_0 > 1$ and $R_1 > 1$, which is in full agreement with Theorem 4.4.

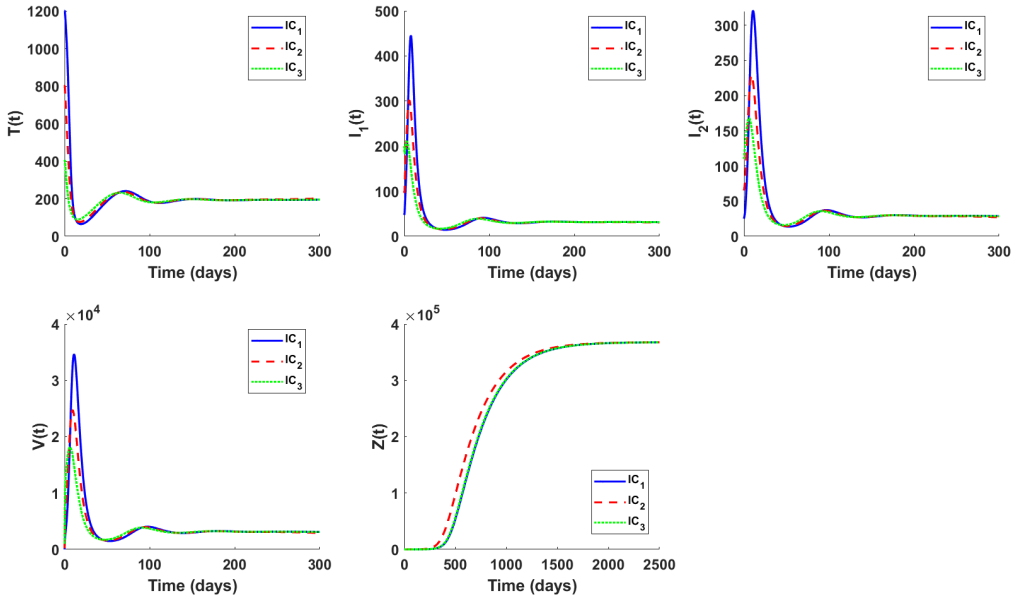

Figure 3. The infection dynamics illustrating the stability of the infected equilibrium with immunity E^*.

6. Sensitivity analysis and drug efficacy

In this section, we conduct a global sensitivity analysis using the LHS-PRCC method [19, 20] to identify the key parameters that influence R_0, R_1 and to simulate the system dynamics under different drug efficacy conditions.

6.1. Sensitivity analysis

The basic reproduction number (R_0) and the CTL immune reproduction number (R_1) are crucial to predict the dynamics of HIV infection. In this section, we employed the LHS-PRCC method to perform a global sensitivity analysis and identify the model parameters that most significantly influence R_0, R_1. We adopted the following classification criteria based on the absolute value of the PRCC: strong correlation for $|PRCC| > 0.5$, moderate correlation for $0.3 < |PRCC| \leq 0.5$, and weak correlation for $|PRCC| \leq 0.3$. Assuming all parameters follow a uniform distribution, we generated 1000 sample values for each parameter within the ranges specified in Table 2 using LHS. The central (baseline) values of these ranges are also listed in the same table for reference.

Figure 4 shows that the basic reproduction number R_0 is most sensitive to the parameters η, k, N, λ, and c, with corresponding PRCC values of -0.92, 0.87, 0.76, 0.78, and -0.61, respectively. Consistent with their PRCC signs, N, k, and λ are positively correlated with R_0, whereas η, c, the natural death rate of target cells (d), and the clearance rate of infected cells (α) are negatively correlated. Notably, the parameters with the strongest influence ($|PRCC| > 0.5$) are primarily associated with viral infection and clearance (the infection rate k, viral clearance rate c, drug efficacy η, and burst size N) and target cell supply (recruitment rate λ and natural death rate d). In contrast, parameters related to the latent reservoir and the death rate of productively infected cells show weaker correlations. These

findings indicate that in model (2.1), the dynamics of HIV infection are predominantly governed by the processes of target cell availability, viral infection, and clearance. Consequently, maintaining a high drug efficacy (η) through consistent medication adherence emerges as a critical factor for suppressing R_0 and aiding immune recovery.

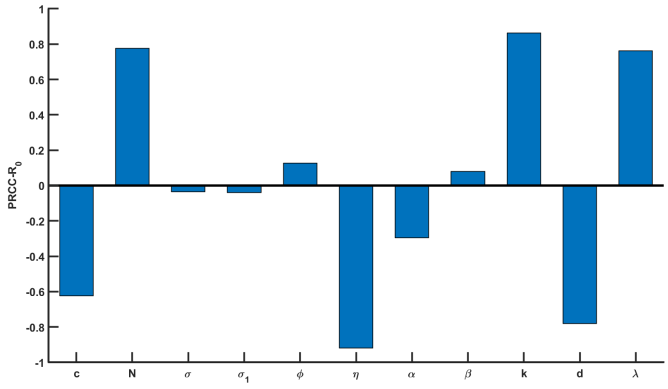

Figure 4. Sensitivity analysis of R_0 with respect to key parameters.

Figure 5 shows that the CTL immune reproduction number R_1 is most sensitive to the CTL-related parameters: The production rate q (PRCC = 0.96) and the death rate b (PRCC = –0.92). Other notable influences include the death rate of productively infected cells σ (PRCC = –0.68) and the recruitment rate of target cells λ (PRCC = 0.47). Overall, the parameters that promote CTL activity or survival (q, λ) are positively correlated with R_1, whereas those that limit it (b, σ) or enhance viral clearance (η, c) are negatively correlated. The dominant influence of q and b underscores that, once the immune response is activated, the balance between CTL proliferation and survival becomes the critical determinant of whether the immune system can effectively control the infection.

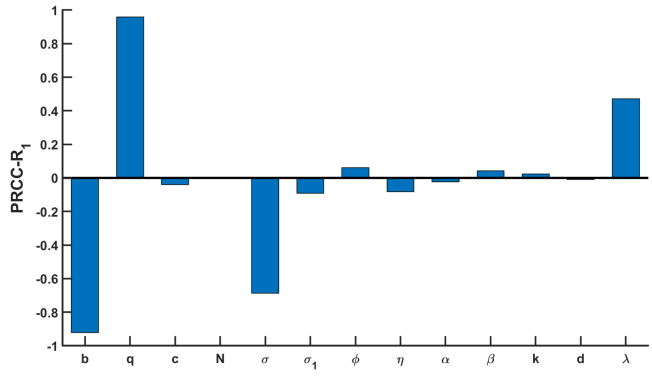

Figure 5. Sensitivity analysis of R_1 with respect to key parameters.

6.2. Drug effects

We analyzed the effect of drug therapy, represented by the parameter η, through numerical simulations. The model tracks the dynamics of uninfected CD4$^+$ T cells (T), Pre-RT infected cells (I_1), Post-RT infected cells (I_2), viral load (V), and CTL cells (Z). The simulations

employed three different initial conditions: $IC_1 = (1200, 50, 25, 1, 0.1)$, $IC_2 = (800, 100, 65, 200, 1)$, and $IC_3 = (400, 200, 110, 1000, 0.5)$. We used the following parameter set: $\lambda = 14$, $d = 0.012$, $k = 3.8 \times 10^{-5}$, $\sigma_1 = 0.016$, $\beta = 1.8 \times 10^{-5}$, $\alpha = 0.038$, $\phi = 0.45$, $\sigma = 0.25$, $p = 3.0 \times 10^{-6}$, $N = 1600$, $c = 2.5$, $b = 0.006$, $q = 2.2 \times 10^{-4}$. To evaluate the effectiveness of the reverse transcriptase inhibitor, we performed simulations for three drug efficacy values: $\eta = 0.3, 0.5, 0.7$. The corresponding basic reproduction numbers were $R_0 = 17.79, 12.7, 7.62$, and the immune reproduction numbers were $R_1 = 1.84, 1.77, 1.59$, respectively. As shown in Figure 6, the therapeutic efficacy (η) substantially influenced the dynamics of all cell populations and the viral load.

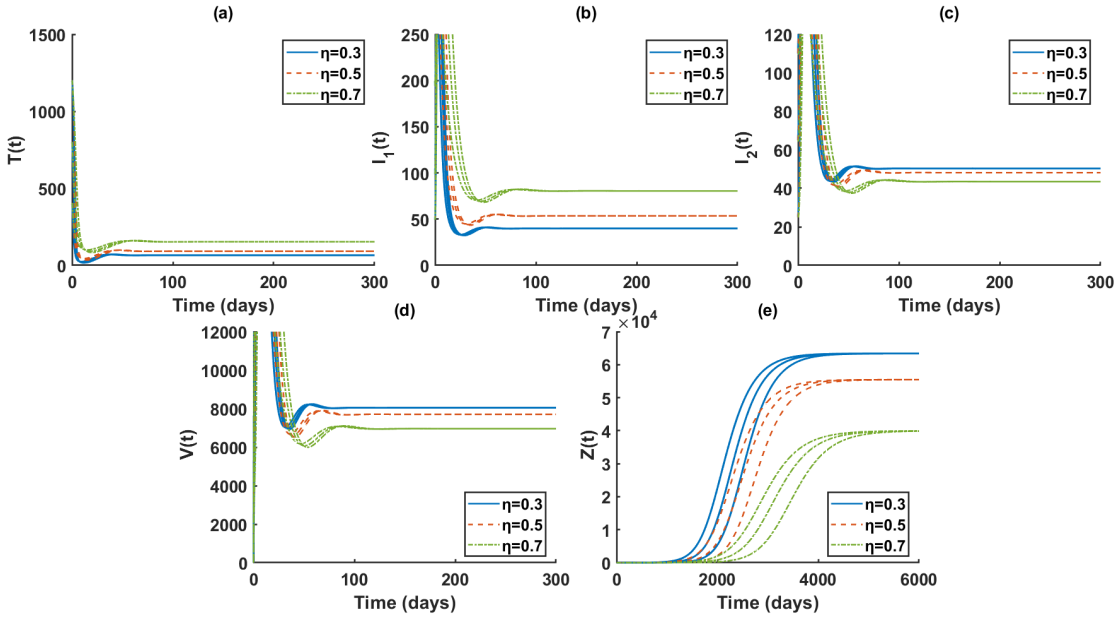

Figure 6. The effects of different drug efficacy levels ($\eta = 0.3, 0.5, 0.7$) on the dynamics of T, I_1, I_2, V, Z.

From a biological perspective, a higher drug efficacy leads to a significant increase in the concentrations of uninfected CD4$^+$ T cells and pre-reverse transcription infected cells. This indicates that reverse transcriptase inhibitors effectively block HIV infection, protect target cells from infection, and inhibit the transition of pre-reverse transcription infected cells to the post-reverse transcription subclass, resulting in an accumulation of the former. Conversely, as the drug efficacy increases, the viral load and the number of cells in the post-reverse transcription subclass decrease substantially. This demonstrates that the inhibitors effectively suppress viral spread by interrupting the infection cascade and eliminating the source of viral production. These results collectively demonstrate that therapeutic effectiveness is paramount to control viral replication and preserve immune function.

7. Conclusions

This study developed an HIV infection model that incorporated CTL immune responses, antiretroviral therapy (ART), Pre-RT infected cells, and Post-RT infected cells capable of producing virus. First, we established the positivity and boundedness of the solutions of model (2.1). Second,

we discussed the existence of equilibria. The basic reproduction number R_0 and the immune reproduction number R_1 determine the dynamical behavior of the system: when $R_0 < 1$, the disease-free equilibrium E_0 is globally asymptotically stable, which implies that the virus will eventually be cleared; when $R_0 > 1$ and $R_1 < 1$, the infected but immune-free equilibrium $\overline{E}$ is locally asymptotically stable, meaning the infection becomes chronic without a successfully activated CTL immune response; and when $R_1 > 1$, the infected equilibrium with immunity E^* is locally asymptotically stable, which indicates a chronic infection with a persistent CTL immune response.

The sensitivity analysis revealed that the drug dosage η is negatively correlated with R_0, thus indicating that reverse transcriptase inhibitors suppress the infection process and inhibit the virus-producing source. This, in turn, increases the concentrations of uninfected cells and Pre-RT infected cells, while decreasing the concentrations of Post-RT infected cells and viral load. Furthermore, when $R_0 > 1$, the CTL immune level declines over time, thus suggesting that chronic HIV infection ultimately leads to immune imbalance.

This model provides a theoretical basis to optimize drug therapy (such as increasing drug efficacy (η) and the recovery rate of infected cells (α)) and target key parameters for intervention (such as viral yield N and infection rate k). In our constructed model, we assumed that only the drug efficacy changes while other parameters remain constant to investigate its effect on the dynamics of T, I_1, I_2, V, and Z. However, in reality, altering the drug efficacy may lead to changes in other parameters, along with the influence of physiological factors such as age, gender, and pathological conditions. How these combined factors affect the dynamics of viral load remains a topic for further study.

It should be noted that our stability analysis has limitations. First, all stability results were local; proving global stability remains an open challenge. Second, the high-dimensional Routh-Hurwitz conditions, while necessary, are algebraically complex and limit biological interpretability. Additionally, model simplifications (linear CTL response, mass-action incidence) may not capture saturation or delays present in vivo. To address these limitations, future work should aim for global stability proofs, incorporate nonlinear functional responses and pharmacokinetics, and explore spatial or stochastic extensions to better reflect biological complexity.

Author contributions

Weimiao Zheng: Writing-original draft, software; Juan Wang: Validation, methodology; Xia Wang: Supervision, writing-reviewing and editing. All authors have read and approved the final version of the manuscript for publication.

Use of Generative-AI tools declaration

The authors declare they have not used Artificial Intelligence (AI) tools in the creation of this article.

Acknowledgments

This work was supported by the National Natural Science Foundation of China (No. 12571548 and No. 12171413).

Conflict of interest

All authors declare that there are no conflicts of interest in this paper.

References

1. *UNAIDS (updated 10 July 2025)*, Available from: https://www.unaids.org/en/resources/fact-sheet.
2. S. Li, C. Moog, T. Zhang, B. Su, HIV reservoir: Antiviral immune responses and immune interventions for curing HIV infection, *Chinese Med. J.*, **135** (2022), 2667–2676. http://dx.doi.org/10.1097/cm9.0000000000002479
3. L. G. Bekker, C. Beyrer, N. Mgodi, S. R. Lewin, S. D. Moretlwe, B. Taiwo, et al., HIV infection, *Nat. Rev. Dis. Primers*, **9** (2023), 1–21. https://doi.org/10.1038/s41572-023-00452-3
4. A. M. Elaiw, E. A. Almohaimeed, A. D. Hobiny, Stability of HIV-8 and HIV-1 co-infection model with latent reservoirs and multiple distributed delays, *AIMS Math.*, **9** (2024), 19195–19239. https://doi.org/10.3934/math.2024936
5. L. Beilina, M. Eriksson, I. Gainova, Time-adaptive determination of drug efficacy in mathematical model of HIV infection, *Differ. Equat. Dyn. Sys.*, **32** (2024), 313–347. https://doi.org/10.1007/s12591-021-00572-w
6. L. Hong, J. Li, L. Rong, X. Wang, Global dynamics of a delayed model with cytokine-enhanced viral infection and cell-to-cell transmission, *AIMS Math.*, **9** (2024), 16280–16296. https://doi.org/10.3934/math.2024788
7. X. Lai, X. Zou, Modeling HIV-1 virus dynamics with both virus-to-cell infection and cell-to-cell transmission, *SIAM J. Appl. Math.*, **74** (2014), 898–917. https://doi.org/10.1137/130930145
8. Y. Huang, X. Meng, X. Wang, L. Rong, Analysis of an HIV latent infection model with cell-to-cell transmission and multiple drug classes, *Appl. Math. Lett.*, **164** (2025), 1–6. https://doi.org/10.1016/j.aml.2025.109478
9. Y. Wang, T. Zhao, J. Liu, Viral dynamics of an HIV stochastic model with cell-to-cell infection, CTL immune response and distributed delays, *Math. Biosci. Eng.*, **16** (2019), 7126–7154. https://doi.org/10.3934/mbe.2019358
10. T. Guo, Z. Qiu, The effects of CTL immune response on HIV infection model with potent therapy, latently infected cells and cell-to-cell viral transmission, *Math. Biosci. Eng.*, **16** (2019), 6822–6841. https://doi.org/10.3934/mbe.2019341
11. W. Wang, G. Wu, X. Fan, Global dynamics of a novel viral infection model mediated by pattern recognition receptors, *Appl. Math. Lett.*, **173** (2026), 1–6. https://doi.org/10.1016/j.aml.2025.109757
12. N. H. AlShamrani, R. H. Halawani, A. M. Elaiw, Stability of generalized models for HIV-1 dynamics with impaired CTL immunity and three pathways of infection, *Front. Appl. Math. Stat.*, **10** (2024), 1–35. https://doi.org/10.3389/fams.2024.1412357
13. A. M. Elaiw, N. H. Alshamrani, Stability of a general CTL-mediated immunity HIV infection model with silent infected cell-to-cell spread, *Adv. Differ. Equ.*, **1** (2020), 1–25. https://doi.org/10.1186/s13662-020-02818-3

14. J. Ren, R. Xu, L. Li, Global stability of an HIV infection model with saturated CTL immune response and intracellular delay, *Math. Biosci. Eng.*, **18** (2021), 57–68. https://doi.org/10.3934/MBE.2021003
15. S. Sutimin, S. Sunarsih, R. Tjahjana, Modeling CD4$^+$T cells and CTL response in HIV-1 infection with antiretroviral therapy, *Commun. Biomath. Sci.*, **1** (2018), 100–109. https://doi.org/10.5614/cbms.2018.1.2.3
16. Y. Yang, R. Xu, Mathematical analysis of a delayed HIV infection model with saturated CTL immune response and immune impairment, *J. Appl. Math. Comput.*, **68** (2022), 2365–2380. https://doi.org/10.1007/s12190-021-01621-x
17. C. Mondal, D. Adak, N. Bairagi, Optimal control in a multi-pathways HIV-1 infection model: A comparison between mono-drug and multi-drug therapies, *Int. J. Control*, **94** (2021), 2047–2064. https://doi.org/10.1080/00207179.2019.1690694
18. Z. Zhang, Y. Chen, X. Wang, L. Rong, Dynamic analysis of a latent HIV infection model with CTL immune and antibody responses, *Int. J. Biomath.*, **17** (2024), 289–316. https://doi.org/10.1142/S1793524523500791
19. S. Marino, I. B. Hogue, C. J. Ray, D. E. Kirschner, A methodology for performing global uncertainty and sensitivity analysis in systems biology, *J. Theor. Biol.*, **254** (2008), 178–196. https://doi.org/10.1016/j.jtbi.2008.04.011
20. T. Guo, Z. Qiu, L. Rong, Analysis of an HIV model with immune responses and cell-to-cell transmission, *B. Malays. Math. Sci. So.*, **43** (2020), 581–607. https://doi.org/10.1007/s40840-018-0699-5
21. P. K. Srivastava, M. Banerjee, P. Chandra, Modeling the drug therapy for HIV infection, *J. Biol. Syst.*, **17** (2009), 213–223. https://doi.org/10.1142/S0218339009002764
22. J. A. Zack, A. M. Haislip, P. Krogstad, I. S. Chen, Incompletely reverse-transcribed human immunodeficiency virus type 1 genomes in quiescent cells can function as intermediates in the retroviral life cycle, *J. Virol.*, **66** (1992), 1717–1725. https://doi.org/10.1128/jvi.66.3.1717-1725.1992
23. X. He, M. Aid, J. D. Ventura, E. Borducchi, M. Lifton, J. Liu, et al., Rapid loss of CD4$^+$ T cells by pyroptosis during acute SIV infection in rhesus macaques, *J. Virol.*, **96** (2022), 1–13. https://doi.org/10.1128/jvi.00808-22
24. W. M. Hirsch, H. Hanisch, J. P. Gabriel, Differential equation models of some parasitic infections: Methods for the study of asymptotic behavior, *Commun. Pur. Appl. Math.*, **38** (1985), 733–753. https://doi.org/10.1002/cpa.3160380607
25. E. X. DeJesus, C. Kaufman, Routh-Hurwitz criterion in the examination of eigenvalues of a system of nonlinear ordinary differential equations, *Phys. Rev. A*, **35** (1987), 1–5. https://doi.org/10.1103/PhysRevA.35.5288

AIMS Press